View metadata, citation and similar papers at core.ac.uk

brought to you by CORE

provided by PolyU Institutional Repository

AIP | Physics of Fluids

Interference between stationary and vibrating cylinder wakes

W. C. Lai, Y. Zhou, R. M. C. So, and T. Wang

Citation: Phys. Fluids **15**, 1687 (2003); doi: 10.1063/1.1569918

View online: http://dx.doi.org/10.1063/1.1569918

View Table of Contents: http://pof.aip.org/resource/1/PHFLE6/v15/i6

Published by the American Institute of Physics.

Related Articles

A new unstable mode in the wake of a circular cylinder
Phys. Fluids 23, 121701 (2011)

Coupling modes of three filaments in side-by-side arrangement
Phys. Fluids 23, 111903 (2011)

Effect of turbulence on the downstream velocity deficit of a rigid sphere
Phys. Fluids 23, 095103 (2011)

Numerical investigation of the subcritical effects at the onset of three-dimensionality in the circular cylinder wake
Phys. Fluids 23, 094103 (2011)

Alternating half-loop shedding in the turbulent wake of a finite surface-mounted square cylinder with a thin boundary layer
Phys. Fluids 23, 095101 (2011)

Additional information on Phys. Fluids

Journal Homepage: http://pof.aip.org/

Journal Information: http://pof.aip.org/about/about_the_journal

Top downloads: http://pof.aip.org/features/most_downloaded

Information for Authors: http://pof.aip.org/authors

ADVERTISEMENT

Downloaded 22 Feb 2012 to 158.132.161.52. Redistribution subject to AIP license or copyright; see http://pof.aip.org/about/rights_and_permissions

Interference between stationary and vibrating cylinder wakes

W. C. Lai, Y. Zhou,[a] R. M. C. So, and T. Wang
Department of Mechanical Engineering, The Hong Kong Polytechnic University, Hung Hom, Kowloon, Hong Kong

(Received 22 March 2002; accepted 5 March 2003; published 5 May 2003)

The flow behind two side-by-side tubes of identical diameter, d, one stationary and the other forced to oscillate in the lateral direction at an amplitude of $A=0.1\sim0.5d$ was examined. Two values of T/d, i.e., 2.2 and 3.5 were investigated, where T is the cylinder center-to-center spacing. The Reynolds number Re ranges from 150 to about 1000. The effect of A/d, T/d, and f_e/f_s, where f_e is the cylinder oscillating frequency and f_s is the vortex shedding frequency of an isolated stationary cylinder, on the vortex shedding and the wake structure was examined. Specific attention was given to the occurrence of lock-in, where vortex shedding from the oscillating cylinder synchronizes with f_e. Significant influence of these parameters has been observed on the flow behind the cylinders in terms of the predominant vortex patterns and interactions between vortices. It has been found that the shedding frequency associated with the oscillating and the stationary cylinder can be modified as f_e/f_s approaches unity. Furthermore, the flow regime may change under the conditions of $T/d=2.2$ and $A/d=0.5$ from two distinct coupled streets to the combination of one narrow and one wide street. Subsequently, the lock-in state is considerably extended probably because multiple dominant frequencies in the asymmetrical flow regime can all be locked in with the structural oscillation. © *2003 American Institute of Physics.* [DOI: 10.1063/1.1569918]

I. INTRODUCTION

The wake of a vibrating structure has received considerable attention in the literature because of its practical significance. One of the primary concerns is that the vortex-shedding frequency from a vibrating structure may synchronize with the natural frequencies of the fluid-structure system, which amplifies structural vibration amplitude and leads to a reduced lifespan of the structure or even early failure. Furthermore, the wake of one or more vibrating structures is of relevance to the prediction of forces on downstream structures.

In their early studies of a single forced oscillating cylinder in a cross flow, Bishop and Hassan[1] observed that when the cylinder oscillating frequency f_e approached the vortex shedding frequency f_s of a stationary cylinder, the two sets of forces were synchronized, and the natural shedding frequency was lost, resulting in the so-called lock-in phenomenon. Within the synchronization range, lift and drag forces varied in phase and amplitude with the imposed frequency. Koopmann[2] noted that the lock-in range, over which the vortex shedding frequency was dictated by f_e, was dependent on the amplitude ratio A/d and, to some extent, on the Reynolds number Re (based on d and the free stream velocity U_∞). The vortex shedding frequency could vary up to $\pm25\%$ for the same Re (<300). Griffin *et al.*[3,4] found that the lock-in occurred for $f_e=0.8-1.2f_s$. They further observed that, due to the forced vibration effect, the lateral spacing between vortices decreased as A/d increased but the longitudinal spacing was unchanged. Williamson and Roshko[5] discussed various spatial modes of vortices, generated by a vibrating cylinder at different A/d and f_e/f_s. Ongorem and Rockwell[6,7] investigated at various f_e/f_s the phase shift, recovery and mode competition in the near-wake for an oscillating cylinder of different cross sections (circular, square, and triangular). They noted that when $f_e/f_s\approx1$, the vortex formation timing switched phase by almost 180° over a very narrow range of f_e. Numerical studies have also been conducted. For example, using a primitive-variable formulation on a spectral element spatial discretization, Blackburn and Henderson[8] simulated a two-dimensional flow past a circular cylinder that was either stationary or in simple harmonic cross-flow oscillation at Re=500, $A/d=0.25$, and $f_e/f_s=0.875-0.975$. They showed that the change in phase of vortex shedding is associated with a change in sign of mechanical energy transfer between the cylinder and the flow.

Previous studies have greatly improved our understanding of the flow behind a vibrating cylinder. In engineering, however, we are frequently faced with the problem of multiple vibrating cylinders instead of an isolated one. Numerous investigations have been conducted to understand the cylinder wake in the presence of a neighboring cylinder. It is now well known that, when the cylinder center-to-center spacing ratio T/d is greater than 2, two distinct vortex streets occur behind the cylinders. The two streets are predominantly in antiphase mode.[9] Nevertheless, the in-phase vortex streets are also observed form time to time.[10–12] The critical points, such as vortex centers and the saddle points,[13] of the two in-phase streets are antisymmetrical about the flow centerline, but symmetrical for the antiphase case. At $1.5\lesssim T/d\lesssim2.0$, the gap flow between the cylinders is deflected, forming one narrow and one wide wake.[10,14] The deflected gap

[a]Author to whom correspondence should be addressed. Electronic mail: mmyzhou@polyu.edu.hk

 © 2003 American Institute of Physics

Downloaded 22 Feb 2012 to 158.132.161.52. Redistribution subject to AIP license or copyright; see http://pof.aip.org/about/rights_and_permissions

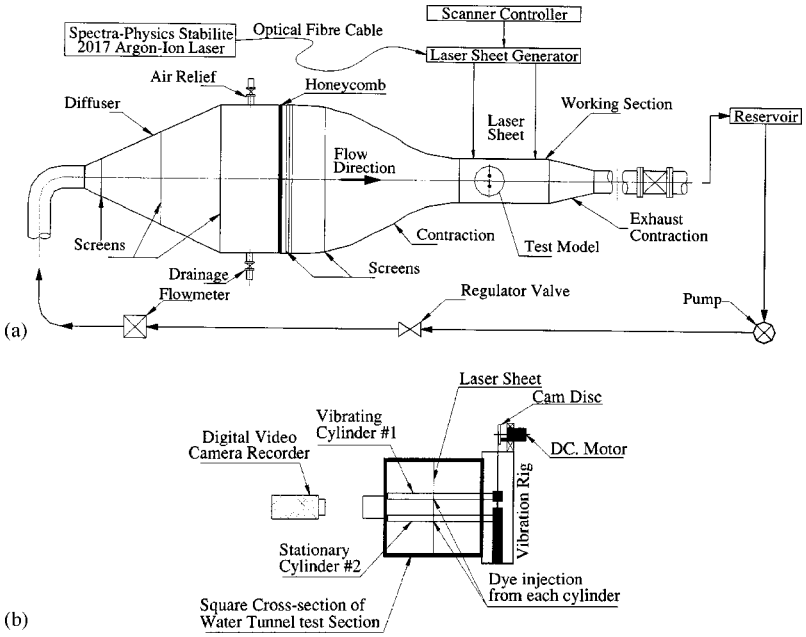

FIG. 1. (a) Schematic diagram of the water tunnel. (b) Cylinder arrangement in the test section.

flow may change over intermittently from one side to another and is bi-stable. For very small spacing ratio, i.e., $T/d < 1.2$, vortices are alternately shed from the free-stream side only of the two cylinders, generating one single vortex street. Mahir and Rockwell[15] investigated the wake of two side-by-side cylinders ($T/d = 3.0$), both forced to vibrate laterally. In the lock-in state, they observed a variety of flow patterns, which depended on the phase relationship between the two vibrating cylinders. The power spectral density function corresponding to the flow patterns was nevertheless almost the same. However, information on the flow when the neighboring cylinder is vibrating is scarce.

This work aims to investigate interference between a stationary and a vibrating cylinder wake based on particle image velocimetry (PIV), hot wires, and laser-induced fluorescence (LIF) flow visualization measurements. Great attention was given to the occurrence of lock-in. Various parameters, including A/d, T/d, and f_e/f_s, are investigated of their influence on the flow behind the cylinders in terms of the predominant vortex patterns, shedding frequencies and interactions between vortices.

II. EXPERIMENTAL DETAILS

A. Flow visualization in a water tunnel

Experiments were carried out in a water tunnel with a square working section (0.15 m×0.15 m) of 0.5 m long. The water tunnel is a recirculating single reservoir system [Fig. 1(a)]. A centrifugal pump delivers water from the reservoir to the tunnel contraction. A honeycomb is used to remove any large-scale irregularities prior to the contraction. The flow speed, controlled by a regulator valve, is up to a maximum of about 0.32 m/s in the working section. The working section is made up of four 20 mm thick Perspex panels.

Two side-by-side acrylic circular tubes of an identical diameter $d = 0.01$ m, were horizontally mounted 0.20 m downstream of the exit plane of the tunnel contraction and placed symmetrically about the midplane of the working section [Fig. 1(b)]. The cylinders were cantilevered; there was a 1 mm or so clearance between the cylinder free end and the tunnel wall. The resulting blockage was about 13%. The relatively high blockage may postpone the near-wake instability to a higher Re and further lead to the wake narrowing and subsequently rising Strouhal number,[16] which are not the focus of the present investigation. Therefore, no correction was made for the blockage effect. The upper cylinder oscillated vertically at $A/d = 0.1$ and 0.5, respectively. The oscillation was provided by a dc motor through a cam-linkage system. The oscillation frequency, f_e, was measured by a tachometer (accuracy: $\pm 5\%$) and confirmed by counting cylinder oscillation when playing back the real-time indexed video record. The f_e/f_s investigated varied between 0.74 and 1.44. In this paper, f_s denotes the vortex shedding frequency of a single stationary cylinder (measured in the same tunnel), while f_{s1} and f_{s2} are the vortex shedding frequencies of the oscillating and the stationary cylinder, respectively.

Two transverse spacing ratios were used, i.e., $T/d = 3.50$ and 2.20, respectively. For stationary cylinders, three distinct flow regimes occur, depending on the T/d value.[9–12] Two distinct and coupled streets occur at $T/d \geqslant 2$; a bi-stable asymmetrical flow is observed for $1.5 \lesssim T/d \lesssim 2$. It is interesting to see how the coupling is affected when one cylinder oscillates and thus $T/d = 3.5$ was selected. It is equally interesting to see whether the flow regime could be changed, because of the cylinder oscillation, from two distinct coupled streets to the asymmetrical flow regime. Therefore, $T/d = 2.2$ was also investigated.

The cylinders have an aspect ratio of 15. For a stationary cylinder, an aspect ratio of 27 or larger is needed to avoid the end effects.[17] However, an oscillating cylinder may reorganize the vortex shedding process to enhance significantly its two dimensionality. Griffin[18]observed that, when the oscillation amplitude was greater than 0.01–0.02d, the correlation coefficient, ρ_p, between spanwise fluctuating pressures in-

Downloaded 22 Feb 2012 to 158.132.161.52. Redistribution subject to AIP license or copyright; see http://pof.aip.org/about/rights_and_permissions

creased greatly, compared with a stationary cylinder. For example, given a threshold of $\rho_p = 0.5$, the spanwise correlation length was about $1d$ at $A/d = 0.025$, $6d$ at $A/d = 0.075$ and $10d$ at $A/d = 0.125$. For $A/d = 0.5$, the correlation length is estimated to be over $40d$ based on an extrapolation of the data. It may be thus inferred that the end effect of the oscillating cylinder is negligible. Section III will show that vortex shedding from the stationary cylinder is also reorganized by the neighboring oscillating flow, which enhanced the two dimensionality of the flow, implying a small end effect for the stationary cylinder.

For each cylinder, dye (Rhodamine 6G 99%), which had a faint red color and became metallic green when excited by laser, was introduced through two injection pinholes at the midspan of the cylinder. The pinholes were located around 90° away, clockwise and anticlockwise, respectively, from the leading stagnation point. A thin laser sheet, which was generated by laser beam sweeping, provided illumination vertically at the midplane of the working section. A Spectra-Physics Stabilite 2017 argon ion laser with a maximum power output of 4 watts was used to generate the laser beam. A digital video camera recorder (SONY DCR-PC100E) was used to record, at a framing rate of 25 frames per second, the dye-marked vortex streets. Flow-visualization was carried out in the range of Re=150–1000 over $0 \leqslant x/d \leqslant 8$. At larger Re and x/d, the dye diffused too rapidly to be an effective marker of vortices.

B. Experiments in a wind tunnel

Wind tunnel and cylinder assembly: The wind tunnel was described in detail by Zhou *et al.*[19] It has a square working section (0.6 m×0.6 m) of 2.4 m in length. The view window of the working section is made of optical glass in order to maximize the signal-to-noise ratio in PIV measurements. The wind speed in the working section is adjustable in the range of 0–50 m/s. The cylinder assembly was designed similarly to that used for the LIF measurements in the water tunnel. Two aluminum alloy cylinders of $d = 0.015$ m were cantilever-supported symmetrically about the midplane of the working section. Their transverse spacing was adjustable in the range of $T/d = 2–4.5$. The length of both cylinders inside the tunnel was 0.35 m, thus resulting in a blockage of 1.25% and an aspect ratio of about 23. A 0.15 m long section from the free end of each cylinder was replaced by a transparent acrylic tube in order to allow the laser sheet to shine through, thus minimizing the shadow effects in the PIV measurement. One microcomputer-controlled dc motor system was used to drive the upper cylinder to oscillate at $A/d = 0.1–0.5$, and $f_e/f_s \approx 0.5–1.3$. The first-mode natural frequency of each cylinder was about 272 Hz, a factor of 11 times the maximum f_e(=24 Hz). To minimize the reflection noise generated by the laser sheet shining on the cylinders, the surface of both cylinders were painted black except a 0.02 m long section at 0.12 m from the free end on the acrylic section. Measurements were conducted at $U_\infty = 1.17$ m/s (Re=1150). In the free stream, the longitudinal turbulence intensity was measured to be approximately 0.4%.

PIV measurements: A Dantec standard PIV2100 system was used. Flow was seeded by the smoke of a particle size around 1 μm in diameter, which was generated from Paraffin oil. Illumination was provided in the plane of mean shear, 0.13 m from the cylinder free end, by two New Wave standard pulsed laser sources of a wavelength of 532 nm, each having a maximum energy output of 120 mJ. Digital particle images were taken using one CCD camera (HiSense type 13, gain×4, double frames, 1280×1024 pixels). A Dantec FlowMap Processor (PIV2100 type) was used to synchronize image-taking and illumination. Each image covered an area of 129 mm×102 mm or $8.6d \times 6.8d$ of the flow field. The longitudinal and lateral image magnifications were identical, i.e., 0.1 mm/pixel. Each laser pulse lasted for 0.01 μs. The interval between two successive pulses was typically 50 μs. Thus, a particle would only travel 0.059 mm (0.59 pixels or $0.004d$) at $U_\infty = 1.17$ m/s. An optical filter was used to allow only the green wavelength (532 nm), generated by the laser, to pass. Since both cylinders were included in the PIV images, which could cause errors in deriving velocities around the cylinders, they were masked using a built-in masking function in the Dantec PIV2001 system before calculation of particle velocities. In image processing, 32×32 rectangular interrogation areas were used, each including 32 pixels ($\approx 0.2d$) with 25% overlap with other areas in both the longitudinal and lateral directions. The ensuing in-plane velocity vector field consisted of 53×42 vectors. The same number of spanwise vorticity component, ω_z, were approximately derived based on particle velocities. The spatial resolution for vorticity estimate was about 2.43 mm or $0.16d$.

Hot wire and laser vibrometer measurement: The dominant frequencies behind the two cylinders were measured using two hot wires. They were placed at $x = 2d$ downstream of the cylinders and symmetrically about the centerline, i.e., at $y = \pm 2.6$ ($T/d = 2.2$) or ± 3.25 ($T/d = 3.5$). Constant-temperature circuits were used for the operation of the hot wires. The displacement of the upper oscillating cylinder was measured simultaneously with the flow using a Polytec Series 3000 dual beam laser vibrometer.[20] Signals from the hot wires and laser vibrometer were offset, amplified and then digitized using a 16 channel (12 bit) analog/digital board and a personal computer at a sampling frequency $f_{\text{sampling}} = 3.5$ kHz per channel. The typical duration of each record was about 20 s.

III. RESULTS AND DISCUSSION

A. Vortex shedding frequencies

In the case of an isolated cylinder, the lock-in phenomenon occurred for the range of $f_e/f_s \approx 0.7–1.1$ at $A/d \approx 0.7$; this range narrows as A/d reduces.[15] When two inline cylinders were both forced to oscillate laterally in phase, vortex shedding from both cylinders was locked in with oscillation and the f_e/f_s range, where lock-in occurred, was almost the same as its single counterpart; however, if the two cylinders oscillated in antiphase, the range was reduced significantly.[21] When two side-by-side cylinders were both

Downloaded 22 Feb 2012 to 158.132.161.52. Redistribution subject to AIP license or copyright; see http://pof.aip.org/about/rights_and_permissions

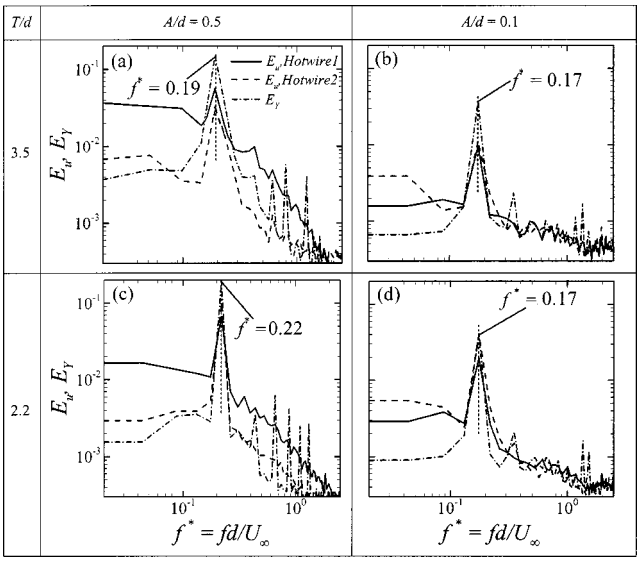

FIG. 2. Power spectral density functions: E_Y of the displacement signal of the oscillating cylinder, E_u obtained at $x/d=2$ and $1.5d$ laterally from the oscillating (hot wire 1) and the stationary cylinder axis (hot wire 2), respectively, towards the free stream. (a) $T/d=3.5$, $A/d=0.5$, $f_e/f_s=0.95$; (b) 3.5, 0.1, 0.85; (c) 2.2, 0.5, 1.15; (d) 2.2, 0.1, 0.85. Re=1150.

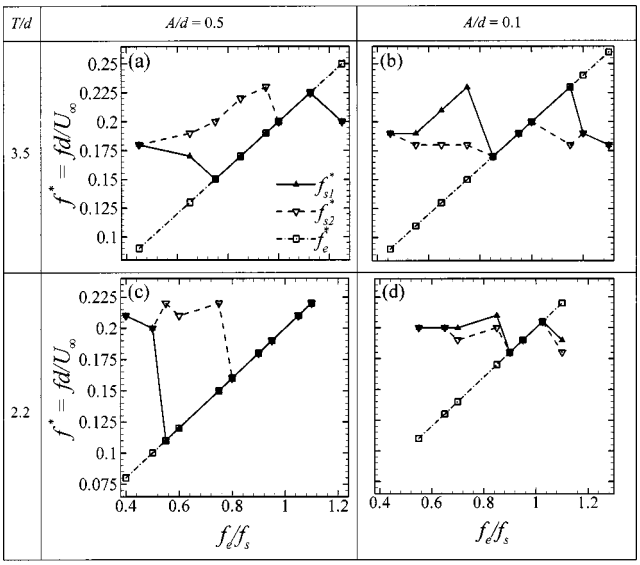

FIG. 3. The vortex shedding frequencies, f_{s1}^* (hot wire 1) and f_{s2}^* (hot wire 2), as f_e/f_s varies: (a) $T/d=3.5$, $A/d=0.5$; (b) 3.5, 0.1; (c) 2.2, 0.5; (d) 2.2, 0.1.

forced to oscillate laterally, the lock-in range of f_e/f_s was narrower, particularly at relatively large A/d, than that of a single cylinder and shifted to a higher f_e/f_s.[15] It is of interest to explore whether vortex shedding from a stationary cylinder could be locked in when the cylinder interacts with a neighboring oscillating cylinder.

Figure 2 illustrates the power spectral density functions, E_u and E_Y, of the hot wire and displacement signals. Note that the displacement signal, Y, monitored the motion of the upper oscillating cylinder, while hot wires 1 and 2 measured the wake of the upper oscillating and lower stationary cylinder, respectively. At $T/d=3.5$ and $A/d=0.5$ [Fig. 2(a)], both E_Y and E_u from hot wire 1 display a pronounced peak at an identical frequency $f^*=fd/U_\infty$, i.e., $f_{s1}^*=f_e^*=0.19$ ($f_e/f_s=0.95$), indicating the lock-in between vortex shedding from the upper cylinder and structural oscillation. Unless otherwise stated, the asterisk denotes normalization by d and U_∞ in this paper. E_u from hot wire 2 also displays a peak at $f_{s2}^*=f_e^*$. Apparently, vortex shedding from the lower cylinder was modified by the neighboring synchronization between f_{s1}^* and f_e^*, its frequency, f_{s2}^*, being thus locked in with f_e^*. As A/d is reduced to 0.1, vortex shedding from the upper cylinder is again locked in with structural oscillation, i.e., $f_{s1}^*=f_e^*$ [Fig. 2(b), $T/d=3.5$, $f_e/f_s=0.85$]. So is vortex shedding from the lower cylinder, resulting in $f_{s2}^*=f_e^*=f_{s1}^*$. Similar observations were made when T/d is reduced to 2.2 [Figs. 2(c) and 2(d)].

Figure 3 compares f_{s2}^* and f_{s1}^* with f_e for different T/d and A/d as f_e/f_s varies. It is evident that in all cases, with f_e/f_s approaching 1, both f_{s2}^* and f_{s1}^* have been modified and eventually collapse with f_e^*. The three frequencies remain synchronized for a range of f_e/f_s, and f_{s2}^* and f_{s1}^* will then be decoupled from f_e^* as f_e/f_s exceeds 1 appreciably. In general, vortex shedding from the stationary cylinder becomes locked in with f_e^* later than that from the oscillating cylinder but decoupled earlier. As expected, the synchronization range of f_e/f_s dwindles for smaller A/d and depends on T/d. Note that at $T/d=2.2$ and $A/d=0.5$, the lock-in range of f_e/f_s is especially wide for oscillating cylinder, starting to occur at $f_e/f_s\approx0.5$. In contrast, the lock-in starts at $f_e/f_s\approx0.8$ for other cases.

At $T/d=2.2$ and $A/d=0.5$, the smallest center-to-center cylinder spacing is 1.7. It is well known that for two side-by-side stationary cylinders of $T/d\leqslant2.0$, the gap flow between the cylinders is deflected, forming one narrow and one wide wake, which are characterized by two dominant frequencies, i.e., $f^*\approx0.3$ and 0.1.[9,10,12] The hot wire spectra (not shown), presently measured in the shear layers around two stationary cylinders of $T/d=1.7$, displayed two peaks at $f^*\approx0.1$ and 0.3. Thus, it seems plausible that the upper cylinder oscillation at a large A/d ($=0.5$) may have excited the shear layer instability at $f^*\approx0.1$, resulting in an early lock-in, as illustrated in Fig. 4. For the same token, the upper cylinder oscillation will probably excite the shear layer in-

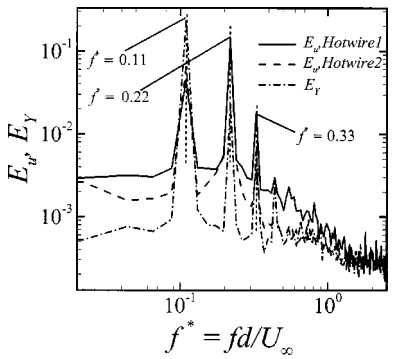

FIG. 4. Power spectral density functions E_Y of the displacement signal of the oscillating cylinder, E_u obtained at $x/d=2$ and $1.5d$ laterally from the oscillating (hot wire 1) and the stationary cylinder axis (hot wire 2), respectively, towards the free stream, $T/d=2.2$, $A/d=0.5$, $f_e/f_s=0.55$. Re=1150.

Downloaded 22 Feb 2012 to 158.132.161.52. Redistribution subject to AIP license or copyright; see http://pof.aip.org/about/rights_and_permissions

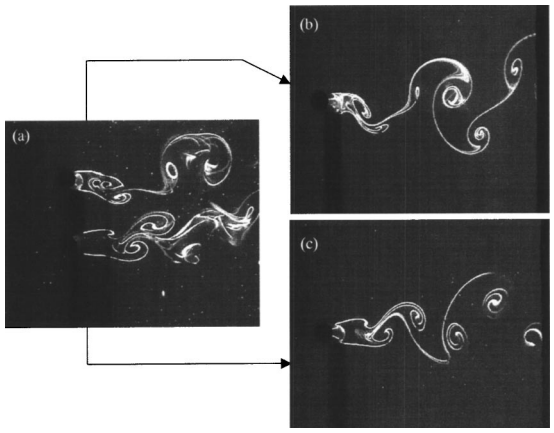

FIG. 5. Comparison between vortex streets behind two cylinders and those behind an isolated cylinder: (a) $T/d=3.5$, $A/d=0.5$, $f_e/f_s=0.83$; (b) an isolated vibrating cylinder, $A/d=0.5$, $f_e/f_s=0.83$; (c) an isolated stationary cylinder. Re=150.

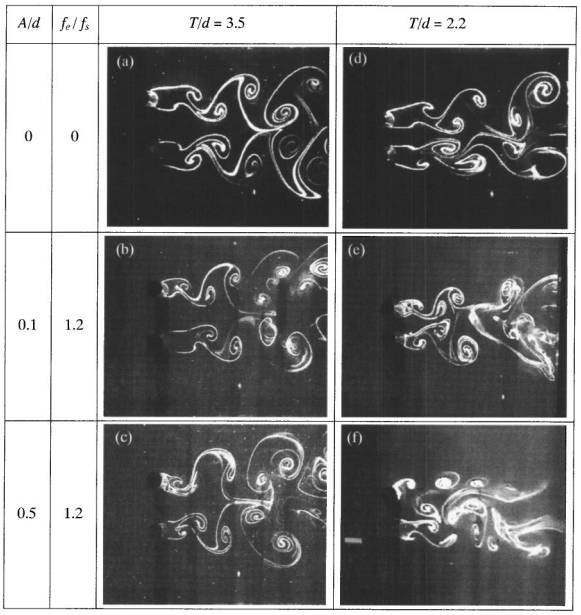

FIG. 6. Vortex streets behind two cylinders at different vibration amplitude: (a) $T/d=3.5$, $A/d=0$, $f_e/f_s=0$; (b) 3.5, 0.1, 1.28; (c) 3.5, 0.5, 1.22; (d) 2.2, 0, 0; (e) 2.2, 0.1, 1.22; (f) 2.2, 0.5, 1.28. Re=150, $f_{s1}=f_{s2}$.

stability at $f^*\approx 0.3$ (the present setup only allowed a maximum f_e/f_s of about 1.3), as suggested by the fact that f^*_{s2} and f^*_{s1} remain synchronized with f^*_e at the upper f_e/f_s. It may be concluded that at $T/d=2.2$ the oscillation of one cylinder, particularly at a large amplitude, acts to reduce effective spacing between cylinders so that the asymmetrical flow behind two side-by-side cylinders may occur above $T/d=2$. The asymmetrical flow regime is characterized by dominant vortex frequencies $f^*\approx 0.3$ and 0.1, respectively. Consequently, lock-in may be inclined to occur near these two frequencies in addition to $f^*\approx 0.2$, leading to a relatively wide lock-in range of f_e/f_s.

Vortex frequencies were also estimated by playing back recorded data from the LIF flow visualization and counting consecutive vortices (about 100 pairs) at $x/d\approx 2$ for a certain period. The measurement uncertainty was estimated to be about 2%. The results (not shown) are essentially consistent with the above observations from spectral analysis.

B. Typical flow structures

At $T/d=3.5$, interference between the two streets appears relatively small in the immediate vicinity, perhaps up to $x/d\approx 5$, of the cylinders. This is illustrated in Fig. 5, where the two vortex streets behind one oscillating and one stationary cylinder [Fig. 5(a)] are compared with that behind a single oscillating [Fig. 5(b)] or stationary cylinder [Fig. 5(c)]. The upper street [Fig. 5(a)] behind the oscillating cylinder appears rather similar to that [Fig. 5(b)] behind the single oscillating cylinder, and the lower street in the near wake of the stationary cylinder resembles that [Fig. 5(c)] behind the single stationary cylinder. The similarity disappears for $x/d\geqslant 5$ as the two streets grow and their interference intensifies, which grossly increases the three dimensionality of the flow.

The two streets behind the cylinders, shown in Fig. 6, are symmetrical about the flow centerline or in the antiphase mode, irrespective of the vibration amplitude of the upper cylinder, as in the stationary cylinder case.[9,10,12] But the in-phase streets are also observed from time to time and can be stable. Furthermore, the oscillation of the upper cylinder tends to increase the wake width as A/d increases. Note that the lateral spacing between vortices generated by the oscillating cylinder will decrease as A/d increases.[3,4] The flow structures in Figs. 6(b) and 6(c) are closely similar to those when both cylinders were forced to oscillate at a phase shift of 0° and 95° observed by Mahir and Rockwell.[15]

As T/d reduces to 2.2 [Figs. 6(d)–6(f)], the interaction between the two streets is expected to intensify, especially for large A/d. For stationary cylinders [Fig. 6(d)], two distinct streets are evident and predominantly symmetrical about the flow centerline. Present data also show the occurrence of in-phase streets (not shown), as previously reported.[10] The two configurations for vortex streets are observed when the upper cylinder oscillates. The effect of cylinder oscillation is dependent on the configurations of vortex streets. For vortex streets in the antiphase mode, the oscillation acts to intensify the vortex interaction and to destabilize the two streets. Consequently, the two streets break up sooner, in particular at small T/d [compare Figs. 6(d), 6(f) with Figs. 6(b) and 6(c)]. On the other hand, the two streets in phase typically start to merge into one at a downstream distance close to the cylinders (see the following section for more details). The above typical flow structures were also observed for a higher Re (up to 1000 in the present LIF flow visualization data) in the turbulent flow regime (not shown), indicating an independence of Re in the range examined.

One vortex street in Figs. 6(e) and 6(f) appears rather narrow, compared with the other. This is more evident at $A/d=0.5$ [Fig. 6(f)], in support of the earlier proposition that the cylinder oscillation could reduce effective spacing between cylinders, thus causing the formation of one narrow and one wide wake even at $T/d=2.2$.

The typical flow structures observed in flow visualiza-

Downloaded 22 Feb 2012 to 158.132.161.52. Redistribution subject to AIP license or copyright; see http://pof.aip.org/about/rights_and_permissions

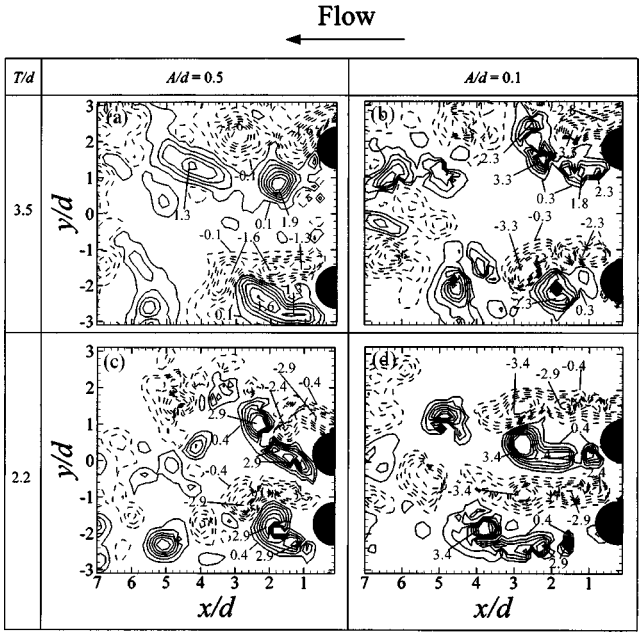

FIG. 7. Instantaneous vorticity contours $\omega_z^* = \omega_z d/U_\infty$ obtained for the PIV measurement: (a) $T/d=3.5$, $A/d=0.5$, the contour increment=0.3; (b) 3.5, 0.1, 0.5; (c) 2.2, 0.5, 0.5; (d) 2.2, 0.1, 0.5. Re=1150, $f_e/f_s=1$.

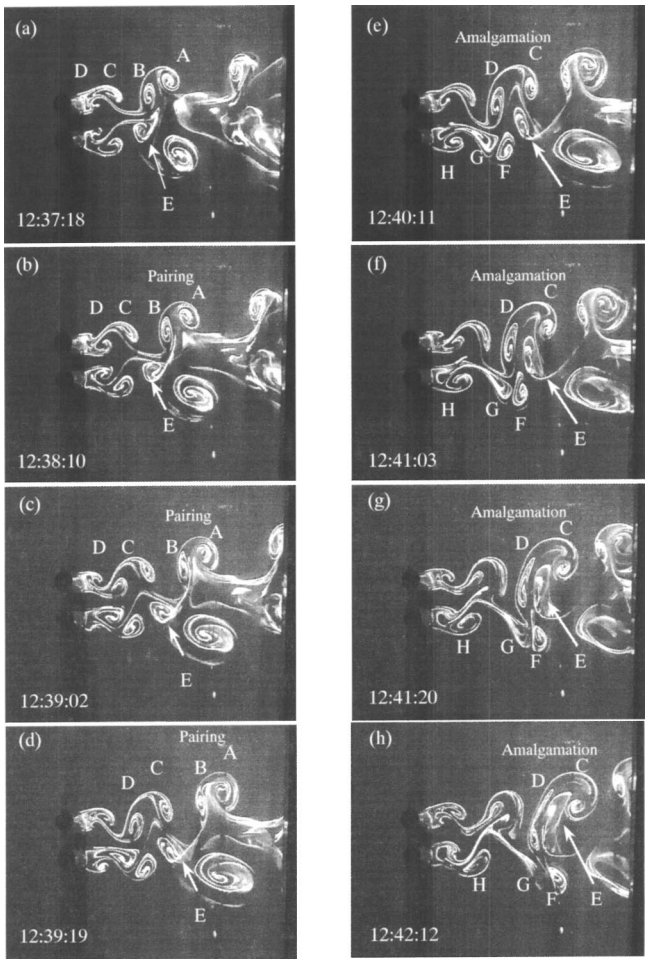

FIG. 8. Sequential photographs of flow visualization: the occurrence of two pairing vortices followed by the merging of two cross-stream vortices shed from the vibrating cylinder with the inner vortex from the stationary cylinder. Meanwhile, symmetrical vortex shedding changes to the antisymmetrical one. $T/d=2.2$, the upper cylinder is vibrating at $A/d=0.1$, $f_e/f_s = f_{s1}/f_s = f_{s2}/f_s = 1.22$, Re=150.

tion were corroborated by vorticity contours, $\omega_z^* = \omega_z d/U_\infty$, deduced from PIV measurements. Figure 7 illustrates the antiphase vortex streets at different T/d and A/d ($f_e/f_s=1$). In all cases, the ω_z^* contours display essentially two vortex streets approximately symmetrical (not in terms of the sign of ω_z^*) about $y/d=0$, but symmetry does not appear evident for $x/d \geqslant 5$. On the other hand, the flow visualization photographs indicate that symmetry persists up to at least about $x/d \approx 8$ for $T/d=3.5$, though not for the case of $T/d=2.2$. At $T/d=2.2$, strong interactions between the two streets quickly destroys the symmetry perhaps even before $x/d=5$. Disparity in the streamwise extent of symmetry at $T/d=3.5$ could be partially ascribed to different Reynolds numbers between the LIF photographs (Fig. 6, Re=150) and PIV data (Fig. 7, Re=1150). It is worthwhile remarking that the two streets at $T/d=2.2$ measured by PIV were more likely to be in-phased than antiphased, which is not quite understood at this stage. The comparison between flow visualization and PIV measurements suggests that the streak lines presently measured reflect reliably the flow structure in the near wake, at least up to $x/d=5$. Therefore, the following discussion of vortex interactions in the near wake will be conducted largely based on the flow visualization data, with a caveat that the streak lines may not follow vortices entirely when far away from the point where dye was released.[22]

C. Change in the phase relation between the two streets

It is of fundamental interest to understand why the two streets may change from antiphase to in-phase. For two side-by-side cylinders of relatively large spacing, i.e., $T/d>2$, two distinct coupled vortex streets occur.[23] Based on flow-visualization data at Re=100–200, Williamson[11] demonstrated that the two streets may occur in phase or in antiphase. The in-phase streets eventually merged downstream to form a single street, while the in-antiphase streets remained distinct farther downstream. He observed a predominant antiphase vortex shedding for $2<T/d<6$. However, it is not clear what triggers the transition of the two vortex streets from antiphase to in-phase or vice versa.

Figure 8 presents sequential photographs for Re=150 and $A/d=0.1$. The real time index is indicated by the first two numbers on the lower left-hand corner in the photographs and the sequential order is given by the third number. The vortex formation from the two cylinders is initially symmetric [Fig. 8(a)]. One gap vortex A generated by the oscillating cylinder approaches the opposite-signed vortex B, which was shed from the free-stream side of this cylinder. It is apparent that A and B are engaged in a pairing process [Figs. 8(a)–8(d)]. Similarly, the following cross-stream vortices C and D also approach each other [Figs. 8(d)–8(g)]. The pair of counter-rotating vortices at close proximity is likely to generate a low-pressure region between them. The low-pressure region is responsible for drawing in the gap

Downloaded 22 Feb 2012 to 158.132.161.52. Redistribution subject to AIP license or copyright; see http://pof.aip.org/about/rights_and_permissions

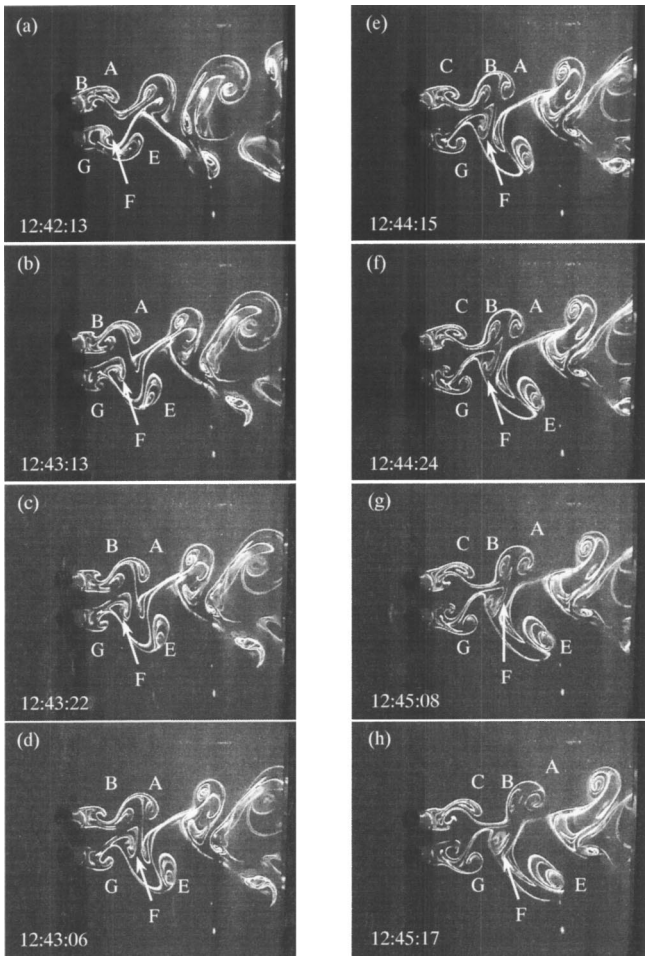

FIG. 9. Sequential photographs of flow visualization: the merging of two cross-stream vortices shed from the vibrating cylinder with the inner vortex from the stationary cylinder. Meanwhile, antisymmetrical vortex shedding changes to the symmetrical one. $T/d=2.2$, the upper cylinder is vibrating at $A/d=0.1$, $f_e/f_s=f_{s1}/f_s=f_{s2}/f_s=1.22$, Re=150.

vortex *E* shed for the lower stationary cylinder, which lags behind *A*, thus resulting in the amalgamation of vortices *C*, *D*, and *E* [Figs. 8(d)–8g)]. Note that the amalgamation of the three vortices acts to slow down vortex *F* and subsequently *G* and *H* [Figs. 8(d)–8(g)]. Eventually, the antisymmetrical vortex formation emerges [Fig. 8(h)] as a result of vortex interactions.

The antisymmetrical vortex shedding did not last long and would soon revert to the symmetrical vortex formation. Sequential photographs (Fig. 9) following those in Fig. 8 indicate that vortices *A* and *B* appear pairing [Figs. 9(d)–9(h)]. Due to the low-pressure region formed between them, *A* and *B* manage to pinch fluid from vortex *F* in the lower street, but they fail to draw in vortex *F*. Apparently, *F* travels at an appreciably slower velocity. Meanwhile, vortices *E* and *F* behind the stationary cylinder appear approaching each other, though not pairing up. This may again produce a low-pressure region between them. Consequently, fluid in the upper street is assimilated to vortex *E* [Figs. 9(b)–9(h)]. This process is associated with a slowdown of the subsequent vortices (e.g., vortices *F* and *G*), thus leading to asymmetric vortex shedding [Fig. 9(h)].

It is interesting to note that the pairing of two vortices or the amalgamation of three vortices leads to the formation of a single vortex street downstream, which is probably asymmetrical. The observation bears resemblance to that behind two stationary cylinders. In the asymmetrical flow regime, i.e., $T/d=1.5$–2.0, where a combination of one wide and one narrow wake occurs, Zhou *et al.*[12] showed the amalgamation of the two cross-stream vortices in the narrow wake with the gap vortex in the wide wake. Subsequently the two streets merge into one. The resemblance further supports the earlier suggestion that the vibration of one cylinder could induce the change of the flow regime from two distinct vortex streets to one wide and one narrow street at a T/d value greater than 2.0.

One remark could be made on the vortex interaction effect on the convection velocity of vortices. In order to highlight this point, a few photographs in Fig. 8 are replotted in Fig. 10. Evidently, the low-pressure region between pairing vortices *C* and *D* draws in and hence slows down *E*. On the other hand, *B* may have been accelerated due to pairing *A* and *B*. Consequently, *B* and *E* were traveled at different velocities. In contrast, the gap vortices, say *A* and *B* in Fig. 11, do not show appreciable difference in their convection velocity when the vortex pairing or amalgamation is absent. Zhou *et al.*[19] measured the turbulent wake ($x/d=10$–40) behind two side-by-side cylinders ($T/d=1.5$ and 3.0) using a three-wire probe (one cold wire plus one X wire). The phase-averaged sectional streamlines and vorticity contours at $T/d=1.5$ showed two rows of vortices, asymmetrically arranged about the flow centerline. The average convection velocity, estimated at $x/d=10$, differed by about 10% between the two rows of vortices. It was, however, not quite clear what was responsible for this difference. The present observation (Figs. 10 and 11) suggests that the interaction between vortices could be partially responsible.

IV. CONCLUSION

The effect of a neighboring vibrating cylinder on a circular cylinder wake has been investigated using particle image velocimetry, hot wires, and laser-induced fluorescence techniques. The dependence of the flow structure and vortex shedding frequencies on f_e/f_s, T/d, and A/d is examined. The following conclusions could be drawn.

(1) For $T/d=3.5$, the vortex shedding frequency f_{s1} of the forced oscillating cylinder can be locked on with the vibration frequency f_e, i.e., $f_{s1}=f_e$, the same as in the case of an isolated cylinder.[3,4] The f_e/f_s range of lock-on is comparable with that for a single cylinder but larger than that for two oscillating side-by-side cylinders.[15] At the lock-in state, the vortex shedding frequency f_{s2} of the stationary cylinder may also be modified, resulting in $f_e=f_{s1}=f_{s2}$. In general, vortex shedding for the stationary cylinder becomes locked in with f_e^* later than that from the oscillating cylinder but decoupled earlier.
(2) When T/d reduces to 2.2, the f_e/f_s range of lock-on increases very significantly at $A/d=0.5$. The cylinder oscillation at such large amplitude acts to reduce effec-

Downloaded 22 Feb 2012 to 158.132.161.52. Redistribution subject to AIP license or copyright; see http://pof.aip.org/about/rights_and_permissions

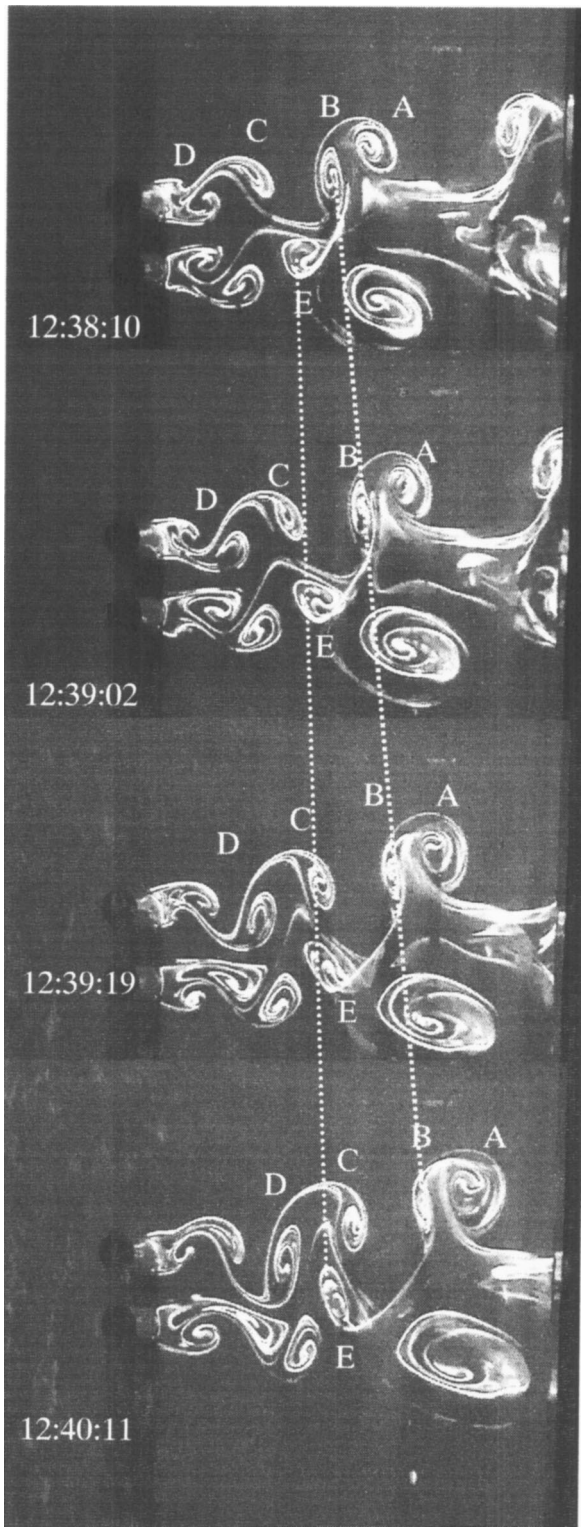

FIG. 10. Sequential photographs of flow visualization: vortex interaction leads to a difference in the convection velocity between the inner vortices shed from the two cylinders. $T/d=2.2$, the upper cylinder is vibrating at $A/d=0.1$, $f_e/f_s=f_{s1}/f_s=f_{s2}/f_s=1.22$, Re=150.

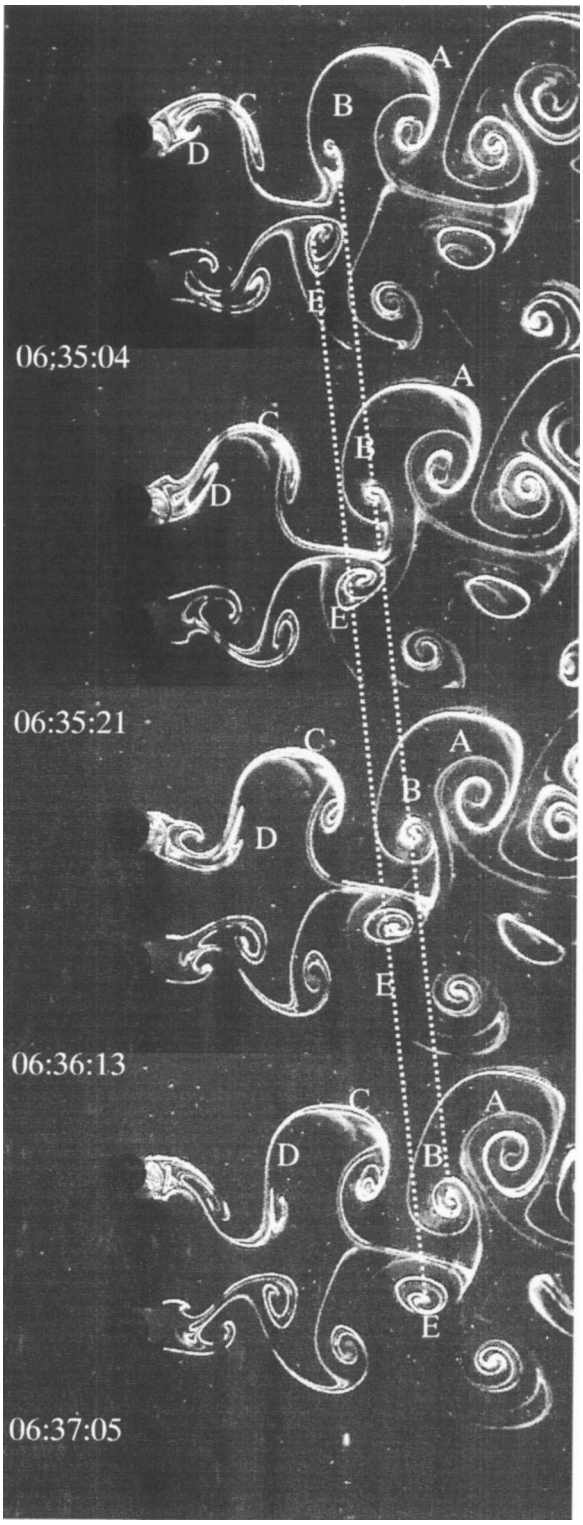

FIG. 11. Sequential photographs of flow visualization: the same convection velocity for the inner vortices shed from the two cylinders. $T/d=3.5$, the upper cylinder is vibrating at $A/d=0.5$, $f_e/f_s=f_{s1}/f_s=f_{s2}/f_s=1.22$, Re=150.

tive spacing between cylinders and to change the flow regime from two distinct vortex streets to one wide and one narrow street. The lock-in of the multiple instability frequencies in the asymmetrical flow regime with the oscillation frequency is probably responsible for the extended lock-in.

(3) At $T/d=2.2$, the two streets do not seem to be stable as a result of the oscillating cylinder. The oscillation effect depends on the mode of vortex streets. For in-antiphase mode streets, the cross-stream inner vortices interact strongly and consequently break up quickly. A single

Downloaded 22 Feb 2012 to 158.132.161.52. Redistribution subject to AIP license or copyright; see http://pof.aip.org/about/rights_and_permissions

street probably emerges further downstream. For in-phase mode streets, the two cross-stream vortices behind the oscillating cylinder tend to pair. The pairing vortices are likely to induce a low-pressure region between them, thus drawing in the gap vortex generated by the stationary cylinder. The amalgamation of the three vortices leads to the formation of a single vortex street downstream, which is probably asymmetrical. The observation is consistent with the occurrence of the asymmetrical flow regime, which has been extended beyond that for the stationary cylinders because of the oscillation of one cylinder.

(4) The amalgamation of the gap vortex shed from the stationary cylinder with two cross-stream vortices generated by the oscillating cylinder acts to slow down the subsequent vortices shed from the stationary cylinder. As a result, the in-antiphase vortex formation changes to the in-phase formation. Similar vortex interaction is associated with the variation from the in-phase vortex formation to the in-antiphase streets.

(5) Two symmetrically formed gap vortices may have been convected at different velocity. The convection velocity of the gap vortex shed from the stationary cylinder was reduced due to the amalgamation of this vortex with two cross-stream vortices generated by the oscillating cylinder. On the other hand, the gap vortex shed from the oscillating cylinder could be accelerated in the process of pairing with the cross-stream outer vortex.

ACKNOWLEDGMENT

The authors wish to acknowledge support given to them by the Central Research Grant of The Hong Kong Polytechnic University through Grant No. G-W009.

[1] R. E. D. Bishop and A. Y. Hassan, ''The lift and drag forces on a circular cylinder oscillating in a flowing fluid,'' Proc. R. Soc. London, Ser. A **277**, 51 (1964).
[2] G. H. Koopmann, ''The vortex wakes of vibrating cylinders at low Reynolds numbers,'' J. Fluid Mech. **28**, 501 (1967).
[3] O. M. Griffin and C. W. Votaw, ''The vortex street in the wake of a vibrating cylinder,'' J. Fluid Mech. **55**, 31 (1972).
[4] O. M. Griffin and S. E. Ramberg, ''The vortex street in the wake of a vibrating cylinder,'' J. Fluid Mech. **66**, 553 (1974).
[5] C. H. K. Williamson and A. Roshko, ''Vortex formation in the wake of an oscillating cylinder,'' J. Fluids Struct. **2**, 355 (1988).
[6] A. Ongoren and D. Rockwell, ''Flow structure from an oscillating cylinder. Part I: Mechanisms of phase shift and recovery in the near wake,'' J. Fluid Mech. **191**, 197 (1988).
[7] A. Ongoren and D. Rockwell, ''Flow structure from an oscillating cylinder. Part II: Mode competition in the near wake,'' J. Fluid Mech. **191**, 225 (1988).
[8] H. M. Blackburn and R. D. Henderson, ''A study of two-dimensional flow past an oscillating cylinder,'' J. Fluid Mech. **385**, 255 (1999).
[9] S. Ishigai, E. Nishikawa, K. Nishmura, and K. Cho, ''Experimental study on structure of gas flow in the tube banks with tube axes normal to flow (Part 1, Karman vortex flow around two tubes at various spacings),'' Bull. JSME **15**, 949 (1972).
[10] P. W. Bearman and A. J. Wadcock, ''The interaction between a pair of circular cylinders normal to a stream,'' J. Fluid Mech. **61**, 499 (1973).
[11] C. H. K. Williamson, ''Evolution of a single wake behind a pair of bluff bodies,'' J. Fluid Mech. **159**, 1 (1985).
[12] Y. Zhou, Z. J. Wang, R. M. C. So, S. J. Xu, and W. Jin, ''Free vibrations of two side-by-side cylinders in a cross flow,'' J. Fluid Mech. **443**, 197 (2001).
[13] Y. Zhou and R. A. Antonia, ''Critical points in a turbulent near-wake,'' J. Fluid Mech. **275**, 59 (1994).
[14] D. Sumner, S. S. T. Wong, S. J. Price, and M. P. Paidoussis, ''Fluid behaviour of side-by-side circular cylinders in steady cross-flow,'' J. Fluids Struct. **13**, 309 (1999).
[15] N. Mahir and D. Rockwell, ''Vortex formation from a forced system of two cylinders: Part II: Side-by-side arrangement,'' J. Fluids Struct. **10**, 491 (1996).
[16] M. M. Zdravkovich, *Flow Around Circular Cylinders* (Oxford University Press, Oxford, 1997), Vol. 1, pp. 38 and 192.
[17] R. King, ''A review of vortex shedding research and its application,'' Ocean Eng. **4**, 141 (1977).
[18] O. M. Griffin, ''OTEC cold water pipe design for problems caused by vortex-excited oscillation,'' NRL Memorandum Report 4157, Naval Research Laboratory, Washington, DC, 1980.
[19] Y. Zhou, H. J. Zhang, and M. W. Yiu, ''The turbulent wake of two side-by-side circular cylinders,'' J. Fluid Mech. **458**, 303 (2002).
[20] Y. Zhou, R. M. C. So, W. Jin, H. G. Xu, and P. K. C. Chan, ''Dynamic strain measurements of a circular cylinder in a cross flow using a fibre Bragg grating sensor,'' Exp. Fluids **27**, 359 (1999).
[21] N. Mahir and D. Rockwell, ''Vortex formation from a forced system of two cylinders: Part I: tandem arrangement,'' J. Fluids Struct. **10**, 473 (1996).
[22] J. N. Cimbala, H. M. Nagib, and A. Roshko, ''Large structure in the far wakes of two-dimensional bluff bodies,'' J. Fluid Mech. **190**, 265 (1988).
[23] L. Landweber, ''Flow about a pair of adjacent, parallel cylinders normal to a stream,'' D. W. Taylor Model Basin, Department of Navy, Report **485**, Washington, DC, 1942.

Downloaded 22 Feb 2012 to 158.132.161.52. Redistribution subject to AIP license or copyright; see http://pof.aip.org/about/rights_and_permissions